Full Paper

Journal of the Brazilian Chemical Society

https://dx.doi.org/10.21577/0103-5053.20260047

J. Braz. Chem. Soc. **2026**, *37-Spe1*, e-20260047, 1-14

Comparative Metabolic Profiling in *Cololobus* Species across Habitats

Marília E. Gallon, [a] ***Marcelo Monge*** [a,b] ***and Norberto P. Lopes*** [*,a]

[a]*Departamento de Ciências BioMoleculares, Faculdade de Ciências Farmacêuticas de Ribeirão Preto, Universidade de São Paulo, 14040-903 Ribeirão Preto-SP, Brazil*

[b]*Programa de Pós-Graduação em Biologia Vegetal, Instituto de Biologia, Universidade de Uberlândia, 38400-902 Uberlândia-MG, Brazil*

As a major biodiversity hotspot, the Atlantic Forest harbors not only an extraordinary richness of species, but also distinct environments, such as inselbergs, where extreme abiotic conditions drive unique ecological and metabolic adaptations. Within the Atlantic Forest biome, the genus *Cololobus*, native to southeastern Brazil, is endemic to inselbergs. With an evolving taxonomic circumscription, the genus remains understudied from a chemical perspective. Herein, we investigated the chemical profiles of *Cololobus* species using liquid chromatography coupled to ultraviolet detection and tandem mass spectrometry (LC-UV-MS/MS) followed by metabolite characterization through *in silico* tools and manual inspection. Comparative analysis of the metabolic profile revealed interspecific variation, with a high prevalence of phenolic compounds, specifically flavonoids and hydroxycinnamic acid derivatives, and sesquiterpene lactones. These metabolites are widely recognized for their ecological functions, including chemical defense against natural enemies and ultraviolet radiation protection, traits likely critical for survival in inselberg habitats. Our results suggest that species from harsher inselbergs are characterized by greater chemical diversity, likely reflecting adaptation to environmental conditions. Taken together, these findings provide insights into metabolic and ecological variation in plants occurring in extreme habitats of the Atlantic Forest.

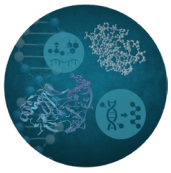

Keywords: LC-MS/MS, metabolite characterization, Asteraceae, Vernonineae, Brazilian biodiversity, natural products

Introduction

The Atlantic Forest is recognized as one of the most biologically diverse biomes in the world.[1-4] Characterized by exceptionally high plant endemism and chemical richness, the biome is currently considered a conservation hotspot.[4] Its distinctive ecological complexity, habitat heterogeneity, and remarkable plant diversity have driven the evolution of a vast repertoire of metabolites, many of which are specific to endemic taxa.[5,6] Despite its outstanding chemical and biological diversity, the Atlantic Forest remains underexplored from a phytochemical perspective, particularly for narrow endemic species and taxa adapted to specialized environments such as inselbergs (i.e., isolated rock outcrops rising abruptly from the surrounding landscape).[7-10] These rock formations are mainly distributed in tropical and subtropical regions, where they act as "terrestrial islands" by creating unique ecosystems that often contain a high number of endemic plant species, which are very distinct environments from the surrounding vegetation matrix.[11,12]

Cololobus is a small genus of subshrubs endemic to inselbergs of the Atlantic Forest.[13,14] The genus *Cololobus* belongs to the tribe Vernonieae and the subtribe Vernoniinae, within the Asteraceae family.[13,14] Currently, the taxon is circumscribed to five described species: *Cololobus argenteus* M.Monge & Semir (2018), *Cololobus hatschbachii* H.Rob. (1994), *Cololobus longiangustatus* (G.M. Barroso) H.Rob. (1994), *Cololobus rupestris* (Gardner) H.Rob. (1994), and *Cololobus ruschianus* M.Monge, Fraga & A.P. Fontana (2021).[15-17] Although the genus was first described approximately three decades ago, its taxonomic circumscription continues to evolve. To date, no studies have investigated the metabolites occurring in *Cololobus* species; therefore, information on their specialized metabolite repertoire and potential chemotaxonomic relevance is lacking. The current absence of phytochemical research represents a notable knowledge gap, particularly considering endemism of the genus to distinctive inselberg

*e-mail: npelopes@fcfrp.usp.br
Editor handled this article: Paulo Wender P. Gomes (Guest)
This publication is part of the special issue "Omics Sciences"

habitats, where unique adaptive chemical traits may have arisen.

In natural products research, metabolite characterization plays an important role in unraveling the chemical diversity of organisms, supporting chemotaxonomic and ecological studies, and guiding the discovery of bioactive compounds.[18-21] Advances in analytical platforms, particularly high-resolution mass spectrometry, nuclear magnetic resonance spectroscopy, and chromatographic techniques, have significantly improved the accuracy and speed of structural elucidation.[22,23] Modern workflows frequently integrate mass spectrometry fragmentation data, molecular networking, *in silico* annotation tools, and reference spectral libraries to facilitate the process of metabolite characterization and enhance confidence levels of annotation.[24,25]

The term metabolite characterization encompasses the assignment of chemical structures to metabolites detected across diverse biological systems (e.g., plants, humans, and microorganisms).[26-28] This process commonly includes putative assignment of a compound based on spectral data and database or *in silico* comparison (referred to as metabolite annotation), as well as unequivocal identification with definitive structural confirmation of a compound relying on authentic reference standards or full spectroscopic elucidation (referred to as metabolite identification).[29,30] Despite the advances in the field, comprehensive metabolite characterization remains a challenge due to structural complexity, stereochemical diversity, and the occurrence of novel or low-abundance metabolites.[24,25,31,32]

Herein, we employed a chemical profiling approach based on liquid chromatography coupled to ultraviolet detection and tandem mass spectrometry (LC-UV-MS/MS) to investigate four *Cololobus* species, namely: *C. argenteus*, *C. longiangustatus*, *C. rupestris* and *C. ruschianus*. By integrating manual curation of chemical spectral data with molecular networking and *in silico* prediction tools for structural elucidation and chemical assignments, we provided a comprehensive chemical characterization of the genus *Cololobus* and established the main differences inter-species. Additionally, we provided insights on the potential ecological roles of these metabolites by examining whether their distribution correlates with the occurrence of the plant across different environments.

Experimental

Plant collection and sample preparation

Leaves of four species belonging to the genus *Cololobus* were sampled from exsiccatae deposited in different Brazilian herbaria, including *Cololobus longiagustatus* (collected by Esgario *et al.* (voucher No. 23), Alto Misterioso, São Roque do Canaã, ES, Brazil: MBML029761), *Cololobus rupestris* (collected by Esgario *et al.* (voucher No. 162), Alto Misterioso, São Roque do Canaã, ES, Brazil: MBML033582), *Cololobus ruschianus* (collected by Monge *et al.* (voucher No. 3320), Mirante do Vale do Canaã, Santa Teresa, ES, Brazil: UEC195464, HUFU), and *Cololobus argenteus* (collected by Monge and Campos-Rocha (voucher No. 3585), Pedra da Tartaruga, Águia Branca, ES, Brazil: HUFU). The herbarium acronyms are in accordance with the Index Herbariorum database.[33,34] Details about each plant material are presented in the Supplementary Information (SI) section, Table S1.

The plants species analyzed in this study were registered in the SisGen website for access to Brazilian genetic heritage in line with the current legislation.

Leaves of each plant species were dried in an oven at 65-70 °C for four days and subsequently stored in a freezer at –8 °C for seven days prior to herbarium deposition. After sampling the herbarium leaves for each species, they were individually pulverized with a mortar and pestle using liquid nitrogen and stored in sealed tubes. For sample preparation, 5 mg of pulverized plant material were weighed into microtubes and 500 µL of MeOH:H_2O solution (7:3, v:v) with hydrocortisone (5 µg mL^{-1}) was added. The microtubes containing the mixture were vortexed (AV-2, Gehaka) for 30 s at room temperature and then placed in an ultrasonic bath (UltraSonic Cleaner 1400, 40 kHz, UNIQUE) for 10 min at room temperature. After the addition of 500 µL of deionized H_2O, the mixtures were centrifuged (M-240R, BOECO, Germany) for 5 min at 10 °C, and the supernatants were filtered through syringe filters with a 0.22 µm polytetrafluoroethylene (PTFE) membrane into vials.

Data acquisition and processing

LC-MS analyses were performed in an ultra-high performance liquid chromatography (NexeraX2, Shimadzu Corporation, Japan) system coupled to a diode array (DAD) ultraviolet detector (SPD-M30A, Shimadzu Corporation, Japan) and to a quadrupole time-of-flight (qTOF) mass spectrometer (LCMS-9050, Shimadzu Corporation, Japan). Volumes of 5 µL of each plant extract were injected in a C18 column (2.6 µm, Polar C18 Kinetex, 100 Å, 150 × 2.1 mm, Phenomenex, Torrance, CA, USA) using a gradient of deionized H_2O (A) and acetonitrile (B) both with 0.1% of formic acid (0-25 min, 10-100% B; 25-27 min, 100% B; 27-28 min, 100-10% B; 28-30 min, 10% B) and a flow rate of 0.3 mL min^{-1}. The oven temperature was set at 40 °C. Data were acquired in positive and negative ionization

modes separately using electrospray ionization in data-dependent acquisition mode. The following parameters were employed in the mass spectrometer: drying and nebulizing gas: nitrogen (N_2); nebulizing gas flow: 3 L min^{-1}; drying gas flow: 10 L min^{-1}; heating gas: dry air; heating gas flow: 10 L min^{-1}; interface temperature: 300 °C; desolvation temperature: 526 °C; desolvation line (DL) temperature: 250 °C; heat block temperature: 400 °C; collision-induced dissociation gas: argon (Ar); number of dependent events: 6; starting delay time: 0.5 s; search *m/z* (mass-to-charge ratio) of precursor ion: 100 to 1500; interaction count of measurements: 3; collision energy: 35 eV; collision energy spread: 20 eV; search for precursor ions: intensity order; precursor intensity threshold: 1000; charge state:, 1-3; select unknown charge state ions; select only monoisotopic; select indeterminable ions; *m/z* range: 100 to 1500 (MS mode) and 50 to 1500 (MS/MS mode); event time: 0.100; maximum loop time: 0.700 s; pulser injection time: 194 μs; Q1 resolution: unit; threshold: low; interface voltage: +3500 V (for positive mode) or –3000 V (for negative mode). The following conditions were employed for the ultraviolet detector: a deuterium (D_2) lamp with positive polarity operating over a wavelength range of 190-700 nm with a spectral resolution of 512 and a slit width of 8 nm.

To allow processing, the data acquired was converted from the proprietary format (.lcd) to an open format (.mzXML) using the Postrun module of the LabSolutions software (Shimadzu Corporation, Japan). Data of positive and negative ionization modes were separately processed. Files in .mzXML format of each corresponding ionization mode were uploaded in the MZmine™ software (version 4.7.27 for Windows, BMC Bioinformatics, United Kingdom) and the following parameters were employed for data processing: mass detection (scan types: all scan types; mass detector: centroid; noise level: 1.0×10^3 for MS level 1 and 1.0×10^2 for MS level ≥ 2); chromatogram builder: scan filter from 0 to 25 min (minimum consecutive scans: 7; minimum intensity for consecutive scans: 1.0×10^3; minimum absolute height: 3.0×10^3; *m/z* tolerance: 0.0050 *m/z* or 10 ppm); smoothing (algorithm: Savitzky-Golay; retention time (t_R) width: 7); local minimum feature resolver (MS/MS scan pairing - MS1 to MS2 precursor tolerance: 0.0100 *m/z* or 25 ppm; retention time filter, use tolerance: 0.2 min - dimension, retention time; chromatographic threshold: 90%; minimum search range t_R: 0.020; minimum relative height: 5%; minimum absolute height: 5×10^3; minimum ratio of peak top/edge: 1.50; peak duration range: 0.05 to 1.50; minimum scans: 7); ^{13}C isotope filter (*m/z* tolerance: 0.0100 *m/z* or 20 ppm; t_R tolerance: 0.10 min; maximum charge: 2; representative isotope: lowest *m/z*); alignment - join aligner (*m/z* tolerance: 0.0050 or 10 ppm; weight for *m/z*: 3; retention time tolerance: 0.20 min; weight for t_R: 1; export molecular networking files (filter rows: MS2 or ion identity; merge and select fragment scans: merged; presets: single scan; merging *m/z* tolerance: 0.0100 or 25 ppm; merge: across samples; intensity merge mode: maximum value; intensity normalization: no normalization; feature intensity: area; CVS export: simple); export for SIRIUS (intensity normalization: no normalization; merge and select fragment scans: merged; presets: representative scan; merging *m/z* tolerance: 0.0100 or 25 ppm; merge: across samples; intensity merge mode: maximum value; *m/z* tolerance: 0.0100 or 20 ppm).

The exported files for Global Natural Product Social Molecular Networking (GNPS) were uploaded to the GNPS2 website[32] to build molecular networks for data obtained in the positive and negative ionization modes separately. The following parameters were employed: feature finding tool: MZmine; precursor ion tolerance: 0.02; fragment ion tolerance: 0.02; window filter: yes; precursor window filter: yes; minimum cosine: 0.65; minimum matched peaks: 4; networking maximum shift: 1999; classic parameter - topK: 10; classic parameter - maximum component size: 100; library minimum cosine: 0.5, library minimum matched peaks: 4; analog search: no; analog search - maximum shift: 1999; top-K: 1; quantification normalization: none. Molecular networks were visualized and interpreted using Cytoscape software (version 3.10.2 for Mac, Institute for Systems Biology, Seattle, WA, USA).

Similarly, the exported files for SIRIUS in the positive and negative ionization modes were separately uploaded to SIRIUS software (version 6.0.3 for Mac, Lehrstuhl Bioinformatik, Jena, Germany) and the following parameters were used: SIRIUS - molecular formula identification; instrument: qTOF; MS2 accuracy (ppm): 10; fallback adducts: $[M + H]^+$, $[M + Na]^+$, $[M + K]^+$, $[M + NH_3]^+$ (for data in the positive ionization mode) and $[M - H]^-$, $[M + CH_2O_2 - H]^-$ (for data in the negative ionization mode); search DBs: all; spectral matching: 20 ppm; perform analog search; molecular formula generation: de novo + bottom up; perform de novo below *m/z* 400; element filter: de novo + bottom up; allowed elements (H, C, N, O, P); autodetect (B, S, Cl, Se, Br); ZODIAC - network-based improved of SIRIUS molecular formula ranking; predict properties - CSI: FingerID - fingerprinting prediction and CANOPUS - compound class prediction: no score threshold; CSI:FingerID - structure database search, no PubChem as fallback; MSNovelist - de novo structure generation. After computing all prediction properties, summaries were exported for the top hit outputs,

which were integrated into the generated molecular networks using Cytoscape software.

All raw LC-MS/MS data (.lcd and .mzXML files), along with the processed data (.mgf files and .csv spreadsheets) employed for molecular networking and SIRIUS predictions, were deposited at the Mass Spectrometry Interactive Virtual Environment (MassIVE) website (see Data Availability Statement section).

Metabolite characterization

After a preliminary overview of the generated molecular networks and SIRIUS metabolite predictions, the total ions chromatograms of each plant species were examined and the MS spectra of the most relevant signals (i.e., peaks with intensity greater than 3,000 ions counts) were manually inspected for metabolite characterization. This thresholding approach ensured analytical robustness and the inclusion of high-quality features while minimizing the influence of background noise and low-abundance artifacts. Molecular formulas were generated for all detected signals using the LabSolutions Insight Explore software (Shimadzu Corporation, Japan). To ensure great accuracy, metabolite characterization was conducted by comparing the molecular features detected in *Cololobus* species with the *m/z* values of metabolites previously described in the tribe Vernonieae.[19,35-43]

Flavonoids were characterized based on their typical ultraviolet (UV) profiles, which generally exhibit two major absorption bands in the ranges of 240-280 and 300-350 nm.[44] More specifically, aglycones moieties were characterized as flavones (showing absorption band at 250-280 and 310-350 nm), flavonols (showing absorption band at 250-280 and 330-360 nm for C3–OH substituted or 350-385 nm for C3–OH free) and flavanones or dihydroflavonols (showing absorption band at 275-295 nm and shoulder at 300-330 nm). The characterization of these aglycones was further supported by MS/MS data and diagnostic *m/z* values: luteolin (*m/z* 287 $[M + H]^+$ and 285 $[M - H]^-$), apigenin (*m/z* 271 $[M + H]^+$ and 269 $[M - H]^-$), luteolin *O*-methyl ether (*m/z* 301 $[M + H]^+$ and 299 $[M - H]^-$), quercetin (*m/z* 303 $[M + H]^+$ and 301 $[M - H]^-$), eriodictyol (*m/z* 289 $[M + H]^+$ and 287 $[M - H]^-$), naringenin (*m/z* 273 $[M + H]^+$ and 271 $[M - H]^-$) and dihydroquercetin (*m/z* 305 $[M + H]^+$ and 303 $[M - H]^-$). Glycosylated forms were recognized by the presence of neutral losses corresponding to hexose (–162 Da) or hexuronose (–176 Da), with no stereochemistry inferred for the sugar moieties.

Similarly, hydroxycinnamic acid derivatives (including caffeoylquinic acids, feruloylquinic acids and coumaroylquinic acids) were characterized based on their ultraviolet absorption features, which typically exhibit maxima in around 325 nm with shoulder in 298 nm.[45] Structural differentiation among these derivatives was supported by their MS/MS patterns, particularly through diagnostic *m/z* values and intensities associated with common substitution patterns.[46,47]

Sesquiterpene lactones were characterized based on their typical UV absorption profiles, which commonly display a strong absorption band at 195-230 nm and a weaker band around 260-280 nm, consistent with the presence of α,β-unsaturated γ-lactone chromophores.[48,49] Their structural elucidation was further supported by diagnostic MS/MS features, particularly low-mass fragments derived from lactone-ring cleavage and neutral losses of water, carbon monoxide, and small alkyl substituents. In the positive ionization mode, these fragmentations produced characteristic ions at *m/z* 277.1071, 259.0965, 241.0859, 231.1016 and 213.0910.[50,51]

Results and Discussion

An outline of the integrative workflow applied for LC-MS/MS data processing, feature selection, and metabolite characterization is shown in Figure 1. Initially, LC-MS/MS data acquired in both positive and negative ionization modes (ESI^+ and ESI^-) were processed to generate lists of features containing MS/MS information. The resulting feature list comprises a broad array of signals, including genuine metabolite ions as well as fragments, adducts, and various analytical artifacts. Therefore, the total ion chromatograms were manually inspected to select the most relevant signals (i.e., those representing true metabolites) for detailed analysis (see SI section, Figures S1 and S2). Through this manual selection process, we refined the dataset to 102 LC-MS/MS-derived signals across the four analyzed *Cololobus* species, each corresponding to a putative metabolite. Among these, 30 features were observed exclusively in the negative ionization mode, 41 exclusively in the positive ionization mode, and 31 in both ionization modes. These findings demonstrate that data analysis in both ionization modes is essential to achieve comprehensive metabolite coverage, as certain compounds ionize preferentially in either the positive or negative mode.

Subsequently, we employed three complementary strategies to advance metabolite characterization: (*i*) *in silico* class assignments using SIRIUS, (*ii*) library-based annotations via GNPS2, and (*iii*) manual interpretation of fragmentation patterns. Manual curation of MS/MS spectra focused on identifying diagnostic ions, thereby enhancing the accuracy of metabolite annotation and

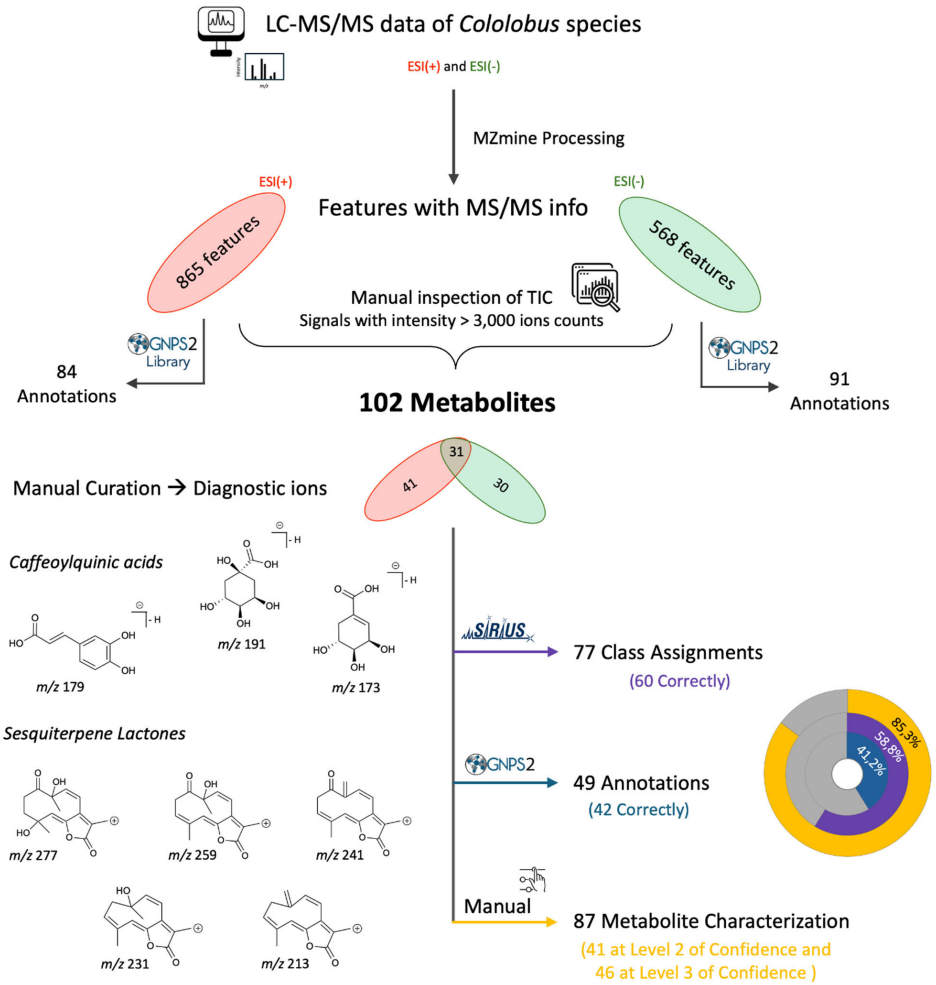

Figure 1. Integrative workflow for LC-MS/MS data processing and metabolite characterization. The final structural proposals were manually inspected (manual curation) based on the rationalization of gas-phase decomposition reactions.

chemical classification. Together, this multistep analytical approach afforded a robust and comprehensive framework for characterizing metabolites across *Cololobus* species.

The predominant metabolites detected across *Cololobus* species were phenolic compounds, including flavonoids and hydroxycinnamic acid derivatives, and sesquiterpene lactones (Table 1). By integrating molecular networking results, *in silico* predictions, and manual curation of MS/MS data, we characterized 41 metabolites at level 2 of confidence (structure-level identification), 46 metabolites at level 3 (class-level assignment) and 15 metabolites at level 4 (molecular formula only) according to the minimum reporting standards for chemical analysis (Table S2, SI section).[29,30] Sesquiterpene lactones were almost exclusively detected in the positive ionization mode, whereas hydroxycinnamic acid derivatives and some flavonoids were more predominantly detected in the negative ionization mode. The fragmentation patterns obtained in the negative ionization mode for hydroxycinnamic acid derivatives provided additional structural information, particularly aiding in determining the positions of phenylpropanoid-derived groups (caffeoyl, feruloyl and coumaroyl units) in the quinic acid moiety.

To enable a comparative assessment of the principal metabolite classes across species and to differentiate metabolites shared among species from those unique to specific taxa, we examined the generated molecular networks, emphasizing the ion-count abundances associated with each species (Figures S3 and S4, SI section).

In general, hydroxycinnamic acid derivatives were detected across all *Cololobus* species (**1**, **5**, **6**, **7N**, **8N**, **10N**, **18**, **21**, **22**, **26** and **34N**). Whereas *C. longiangustatus* exhibited wider variety of hydroxycinnamic acids derivatives, including unique caffeoylquinic acids (**35**, **38** and **51**) and hexose-conjugated phenylpropanoids (**2N**, **3N**, **4N**, **13N**, **15N**, **27N**, **37N** and **45N**) (Figure 2).

Several types of flavonoids were detected, including 14 flavones, 2 flavonols, 5 flavanones and one dihydroflavonols (Figures 3 and 4). In general, flavones apigenin- and luteolin-like aglycones were detected in all *Cololobus* species (**17**,

Table 1. Metabolites detected in *Cololobus* species

ID[a]	t_R / min	Metabolite name and formula	Confidence level	Plant species			
				C. argenteus	*C. longiangustatus*	*C. rupestris*	*C. ruschianus*
1	1.9	3-*O*-Caffeoylquinic acid ($C_{16}H_{18}O_9$)	level 2	●	●	●	●
2N	2.0	Caffeoyl *O*-hexoside ($C_{15}H_{18}O_9$)	level 2		●		
3N	2.2	Caffeoyl *O*-hexoside ($C_{15}H_{18}O_9$)	level 2		●		
4N	2.5	Caffeoyl *O*-hexoside ($C_{15}H_{18}O_9$)	level 2		●		
5	2.6	4-*O*-Caffeoylquinic acid ($C_{16}H_{18}O_9$)	level 2	●	●	●	●
6	2.8	5-*O*-Caffeoylquinic acid ($C_{16}H_{18}O_9$)	level 2	●	●	●	●
7N	4.1	5-*p*-Coumaroylquinic acid ($C_{16}H_{18}O_8$)	level 2	●		●	●
8N	4.3	1,3-*O*-Dicaffeoylquinic acid ($C_{25}H_{24}O_{12}$)	level 2	●	●	●	●
9P	4.7	Apigenin *C*-hexose-hexoside ($C_{27}H_{30}O_{15}$)	level 2		●	●	●
10N	5.0	5-*O*-Feruloylquinic acid ($C_{17}H_{20}O_9$)	level 2		●		●
11N	5.4	Eriodictyol *O*-hexose-*O*-hexuroside ()$C_{27}H_{30}O_{17}$	level 2		●	●	
12	6.1	Dihydroquercetin ($C_{15}H_{12}O_7$)	level 2		●	●	
13N	6.2	Rosmarinic acid *O*-hexoside ($C_{24}H_{26}O_{13}$)	level 2		●		
14	6.4	Eriodictyol *O*-hexuronoside ($C_{21}H_{20}O_{12}$)	level 2		●	●	●
15N	7.2	Rosmarinic acid *O*-hexoside ($C_{24}H_{26}O_{13}$)	level 2		●		
16P	7.5	Putative vernodalinol ($C_{19}H_{22}O_8$)	level 3			●	●
17	7.7	Luteolin *O*-hexuronoside ($C_{21}H_{18}O_{12}$)	level 2	●	●	●	●
18	7.9	3,4-di-*O*-Caffeoylquinic acid ($C_{25}H_{24}O_{12}$)	level 2	●	●	●	●
19P	8.0	Hirsutinolide type-STL ($C_{19}H_{20}O_8$)	level 3	●			●
20	8.1	Naringenin *O*-hexuronoside ($C_{21}H_{20}O_{11}$)	level 2		●	●	●
21	8.2	3,5-di-*O*-Caffeoylquinic acid ($C_{25}H_{24}O_{12}$)	level 2	●	●	●	●
22	8.3	1,5-di-*O*-Caffeoylquinic acid ($C_{25}H_{24}O_{12}$)	level 2	●	●	●	●
23	8.6	Acanthoside B ($C_{28}H_{36}O_{13}$)	level 2	●	●	●	
24	8.9	Apigenin *O*-hexuronoside ($C_{21}H_{18}O_{11}$)	level 2	●	●	●	●
25N	8.7	Luteolin *O*-hexoside ($C_{21}H_{20}O_{11}$)	level 2	●			
26	9.0	1,4-di-*O*-Caffeoylquinic acid ($C_{25}H_{24}O_{12}$)	level 2	●	●	●	●
27N	9.2	Caffeoyl-hexose derivative ($C_{24}H_{24}O_{11}$)	level 2		●		
28P	9.3	Putative vernolepin ($C_{15}H_{16}O_5$)	level 3		●	●	●
29	9.4	Luteolin *O*-methyl *O*-hexuroside ($C_{21}H_{20}O_{11}$)	level 2		●	●	●
30N	9.5	Luteolin *O*-hexoside ($C_{22}H_{20}O_{12}$)	level 2		●	●	
31P	9.5	Luteolin *O*-methyl-*O*-hexoside ($C_{22}H_{22}O_{11}$)	level 2		●	●	
32P	9.6	Putative vernocinerascolide ($C_{19}H_{22}O_8$)	level 3		●	●	●
33	9.7	Eriodictyol ($C_{15}H_{12}O_6$)	level 2		●	●	●
34N	9.9	*O*-Caffeoyl-*O*-feruloylquinic acid ($C_{26}H_{26}O_{12}$)	level 3		●		●
35N	10.1	4,5-di-*O*-Caffeoylquinic acid ($C_{25}H_{24}O_{12}$)	level 2		●		
36P	10.1	Putative hydroxyvernolide ($C_{19}H_{22}O_8$)	level 3		●	●	●
37N	10.2	Caffeoyl-hexose derivative ($C_{26}H_{26}O_{12}$)	level 3		●		
38N	10.3	*O*-Caffeoyl-*O*-feruloylquinic acid ($C_{26}H_{26}O_{12}$)	level 3		●		
39P	10.4	Putative STL ($C_{21}H_{24}O_{10}$)	level 3				●
40P	10.5	Putative dihydrovernodalin ($C_{19}H_{22}O_7$)	level 3		●	●	●
41N	10.5	Luteolin *O*-hexose-hexoside ($C_{30}H_{26}O_{14}$)	level 2		●	●	
42	10.6	Quercetin ($C_{15}H_{10}O_7$)	level 2		●	●	
43P	10.7	Glaucolide-type STL $(C_{23}H_{28}O_1)_1$	level 3				●
44N	10.7	$C_{20}H_{26}O_9$	level 4			●	●
45N	10.8	Flavonoid caffeoyl-hexose derivative ($C_{30}H_{28}O_{14}$)	level 3		●		
46P	10.9	Putative STL ($C_{22}H_{26}O_{10}$)	level 3				●
47	11.0	Luteolin ($C_{15}H_{10}O_6$)	level 2	●	●	●	●

Table 1. Metabolites detected in *Cololobus* species (cont.)

ID[a]	t_R / min	Metabolite name and formula	Confidence level	Plant species			
				C. argenteus	*C. longiangustatus*	*C. rupestris*	*C. ruschianus*
48P	11.2	Putative STL ($C_{20}H_{22}O_9$)	level 3				●
49P	11.3	Putative STL ($C_{19}H_{20}O_7$)	level 3		●	●	●
50	11.3	Quercetin 3-*O*-methyl ether ($C_{16}H_{12}O_7$)	level 2		●	●	●
51N	11.4	3,4,5-tri-*O*-Caffeoylquinic acid ($C_{34}H_{30}O_{15}$)	level 2		●		
52N	11.5	$C_{20}H_{26}O_9$	level 4			●	●
53N	11.6	$C_{33}H_{30}O_{17}$	level 4		●		
54P	11.7	Putative STL ($C_{20}H_{24}O_8$)	level 3			●	●
55P	11.8	Putative STL ($C_{21}H_{24}O_9$)	level 3				●
56P	11.9	Putative STL ($C_{20}H_{22}O_7$)	level 3			●	●
57	12.2	Apigenin ($C_{15}H_{10}O_5$)	level 2	●	●	●	●
58N	12.2	$C_{19}H_{20}O_7$	level 4		●	●	●
59P	12.4	Putative STL ($C_{19}H_{21}O_7$)	level 3		●	●	●
60P	12.6	Putative vernodalin ($C_{19}H_{20}O_7$)	level 3		●	●	●
61P	12.8	Putative STL ($C_{23}H_{26}O_{10}$)	level 3				●
62	13.0	Eriodictyol *O*-methyl ($C_{16}H_{14}O_6$)	level 2		●	●	
63	13.1	Putative STL ($C_{19}H_{21}NO_{10}$)	level 3				●
64	13.3	Tricetin *O*-dimethyl ether ($C_{17}H_{14}O_7$)	level 2	●	●	●	●
65	13.8	Luteolin *O*-methyl ether ($C_{16}H_{12}O_6$)	level 2		●	●	●
66P	14.1	Putative STL ($C_{23}H_{26}O_9$)	level 3				●
67N	14.7	$C_{19}H_{22}O_9$	level 4		●	●	●
68P	14.8	Putative hirsutinolide-type STL ($C_{19}H_{20}O_6$)	level 3	●	●	●	●
69P	15.0	Putative STL ($C_{19}H_{22}O_6$)	level 3		●	●	●
70	15.1	Apigenin *O*-methyl ether ($C_{16}H_{12}O_5$)	level 2	●	●	●	●
71N	15.2	$C_{35}H_{32}O_{13}$	level 4		●	●	
72P	15.4	Putative STL dimer ($C_{34}H_{36}O_{11}$)	level 3		●		
73P	15.5	$C_{38}H_{43}NO$	level 4				●
74	15.6	Putative STL dimer ($C_{38}H_{42}O_{13}$)	level 3		●	●	●
75	15.7	Putative STL dimer ($C_{34}H_{30}O_{13}$)	level 3				●
76P	15.8	Putative STL ($C_{20}H_{22}O_6$)	level 3		●	●	●
77	16.0	Putative STL dimer ($C_{34}H_{30}O_{13}$)	level 3				●
78P	16.4	Putative STL dimer ($C_{42}H_{46}O_{18}$)	level 3				●
79	16.5	Putative STL dimer ($C_{34}H_{30}O_{12}$)	level 3				●
80	16.6	Putative STL dimer ($C_{38}H_{42}O_{13}$)	level 3		●	●	●
81P	16.8	Putative STL dimer ($C_{38}H_{42}O_{14}$)	level 3				●
82P	17.0	Putative STL dimer ($C_{38}H_{40}O_{13}$)	level 3		●	●	●
83P	17.3	Putative vernodalidimer A ($C_{38}H_{40}O_{14}$)	level 3				●
84P	17.4	Putative STL dimer ($C_{39}H_{42}O_{14}$)	level 3				●
85P	17.5	Putative STL dimer ($C_{38}H_{40}O_{13}$)	level 3			●	●
86P	17.6	Putative STL dimer ($C_{38}H_{40}O_{12}$)	level 3		●	●	
87N	17.6	$C_{30}H_{42}O_{11}$	level 4	●		●	●
88	17.7	$C_{35}H_{32}O_{13}$	level 4				●
89P	17.8	Putative STL dimer ($C_{38}H_{40}O_{12}$)	level 3		●	●	
90P	17.8	Putative STL dimer ($C_{37}H_{40}O_{15}$)	level 3				●
91P	17.9	Apigenin *O*-dimethyl ether ($C_{17}H_{14}O_5$)	level 2		●	●	●
92P	18.1	Putative STL dimer ($C_{38}H_{40}O_{12}$)	level 3		●	●	●
93P	18.2	Putative STL dimer ($C_{35}H_{32}O_{12}$)	level 3				●
94P	18.4	Putative STL dimer ($C_{38}H_{40}O_{12}$)	level 3		●	●	●

Table 1. Metabolites detected in *Cololobus* species (cont.)

ID[a]	t_R / min	Metabolite name and formula	Confidence level	Plant species			
				C. argenteus	*C. longiangustatus*	*C. rupestris*	*C. ruschianus*
95N	18.4	$C_{30}H_{44}O_{11}$	level 4	•			•
96N	18.5	$C_{28}H_{48}O_{11}$	level 4	•		•	•
97P	18.6	Putative STL dimer ($C_{38}H_{40}O_{12}$)	level 3		•	•	•
98P	18.7	$C_{27}H_{46}O_9$	level 4	•		•	•
99	18.9	$C_{28}H_{44}O_{11}$	level 4	•	•	•	•
100N	19.5	$C_{36}H_{34}O$	level 4	•			•
101N	20.1	$C_{36}H_{36}O$	level 4	•		•	•
102P	23.3	Putative STL dimer ($C_{35}H_{52}O_9$)	level 3				•

[a]ID refers to peak identification, where P indicates metabolites detected exclusively in the positive ionization mode, N indicates metabolites detected exclusively in the negative ionization mode and numbers alone indicate metabolites detected in both ionization modes. t_R: retention time; STL: sesquiterpene lactone.

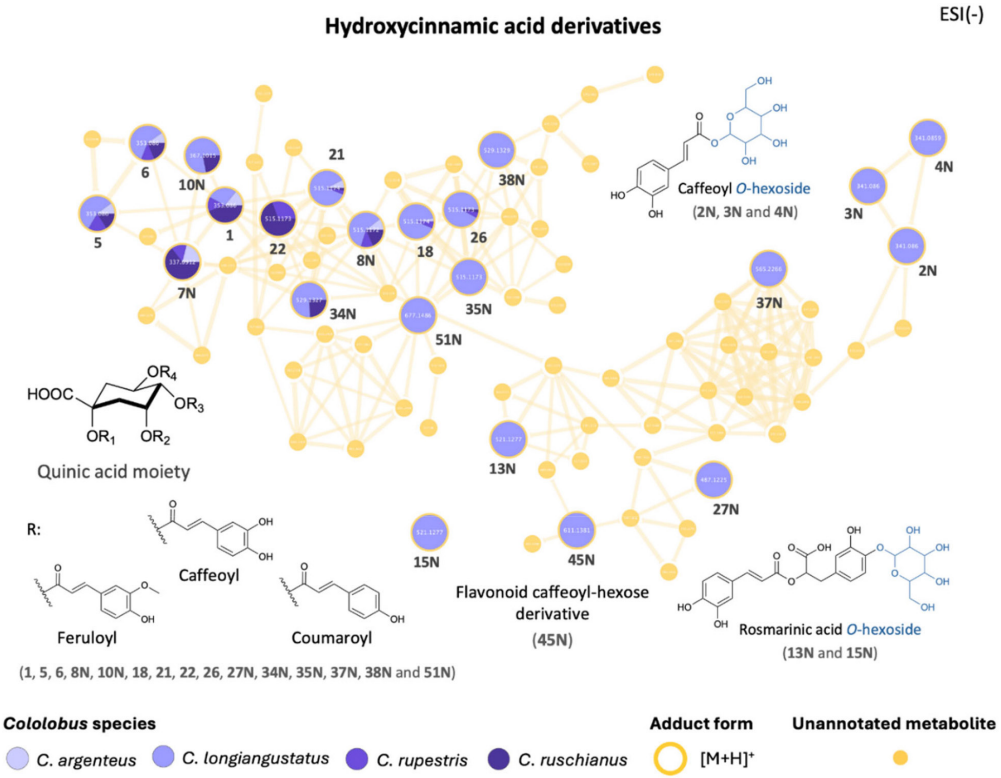

Figure 2. LC-MS/MS molecular networking of *Cololobus* species in the negative ionization mode, highlighting the cluster of metabolites classified as hydroxycinnamic acid derivatives.

24, **47**, **57** and **70**). Interestingly, none of the identified flavonols (**42** and **50**), flavanones (**11N**, **14**, **20**, **33** and **62**) and dihydroflavonol (**12**) were detected in *C. argenteus*. Among the phenolic compounds, the lignan acanthoside B (**23**), a phenylpropanoid derived-metabolite formed by the dimerization of two C_6-C_3, was detected in *C. argenteus*, *C. longiangustatus* and *C. rupestris*, but not in *C. ruschianus*.

A diverse set of sesquiterpene lactones was detected across the *Cololobus* species. Their occurrence varied among taxa and was particularly pronounced in *C. ruschianus* (Figure 5). Several sesquiterpene lactones classified as hirsutinolides, glaucolides and elemanolides were detected in *C. longiangustatus*, *C. rupestris* and *C. ruschianus* (**28P**, **32P**, **36P**, **49P**, **59P**, **60**, **68P** and **76P**), as well as diverse sesquiterpene lactone dimers (**69P**, **74**, **80**, **82P**, **92P**, **94P** and **97P**). In addition, several sesquiterpenes lactones and their dimers were found exclusively in *C. ruschianus* (**39P**, **46P**, **48P**, **55P**, **61P**, **63**, **66P**, **75**, **77**, **78P**, **79**, **81P**, **83P**, **84P**, **90P**, **93P** and **102P**). Interestingly, *C. argenteus* was characterized by the presence of only two sesquiterpene lactones, both classified as hirsutinolides (**19P** and **68P**), displaying markedly fewer sesquiterpene lactones than the other *Cololobus* species. In addition, one putative sesquiterpene lactone (**72P**) was exclusively detected in *C. longiangustatus*.

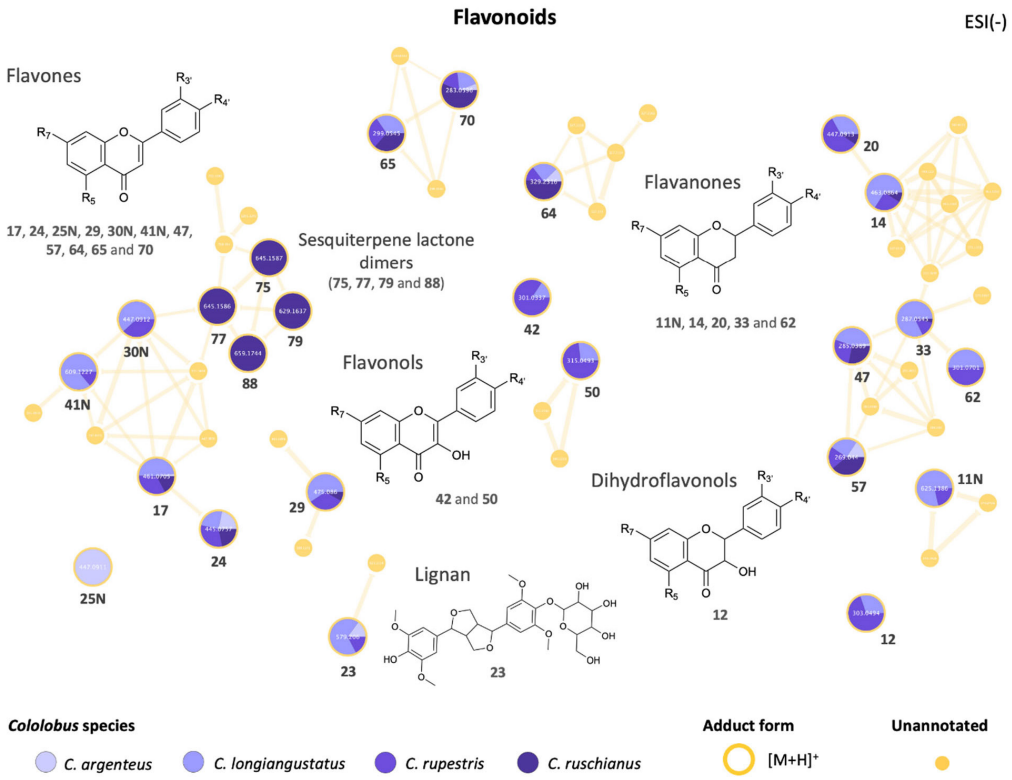

Figure 3. LC-MS/MS molecular networking of *Cololobus* species in the negative ionization mode, highlighting the cluster of metabolites classified as flavonoids and a lignan-type compound.

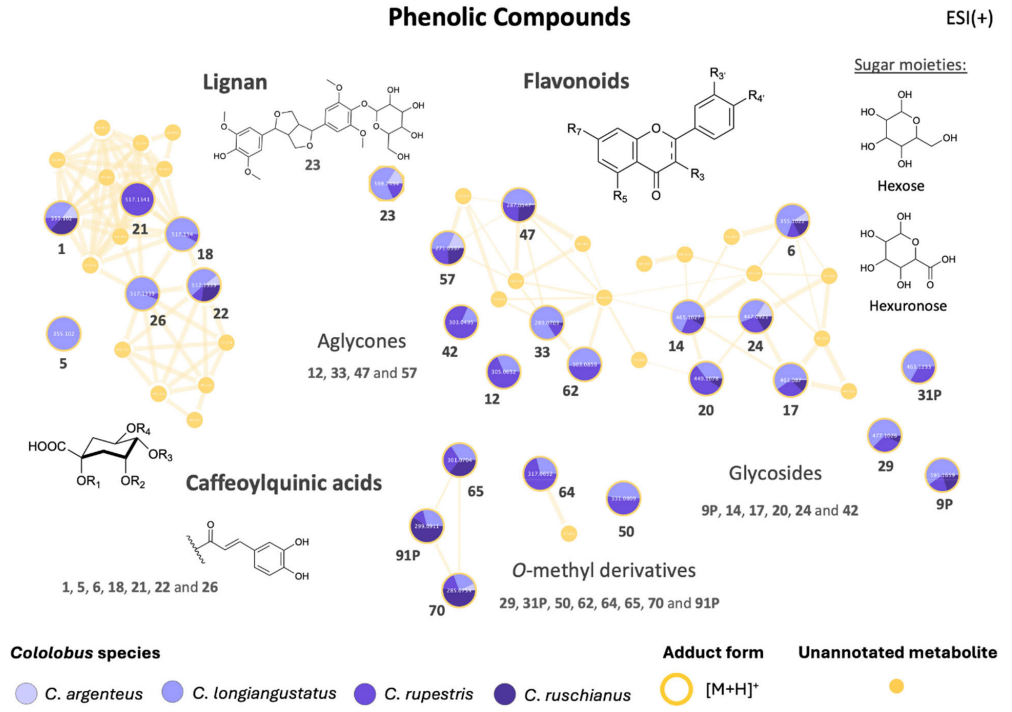

Figure 4. LC-MS/MS molecular networking of *Cololobus* species in the positive ionization mode, highlighting the cluster of metabolites classified as phenolics compounds, including flavonoids and caffeoylquinic acid derivatives, and a lignan-type compound.

The number of detected metabolites varied considerably among species. Specifically, *C. ruschianus* exhibited the highest chemical richness (76 metabolites), followed by *C. longiangustatus* and *C. rupestris* (66 and 63 metabolites, respectively). In contrast, *C. argenteus* displayed the lowest metabolite richness, with 27 detected metabolites

(Figure 6a).

Previous studies[52-57] of Asteraceae species, particularly populations of *Lychnophora* and *Eremanthus*, occurring in the Brazilian "*campos rupestres*" have described the influence of spatial and seasonal factors on the biosynthesis of specialized metabolites. Although both qualitative and quantitative variation have been reported for some populations, major differences were primarily related to metabolite concentration levels. Therefore, from a qualitative perspective, the divergence in metabolic profiles may be associated with environmental variables other than seasonality. Accordingly, our results suggest that the qualitative chemical profiles of *Cololobus* species appear to be influenced by the geographical locations where the plants grow (Figure 6b).

Specifically, *C. argenteus* was collected in the northern region of Espírito Santo state (18°58'59.2"S, 40°44'25.1"W) and exhibited a less diverse chemical profile. *C. argenteous* was sampled at a locality characterized by a drier climate, higher mean annual temperature (23 °C) and lower altitude (142 m above sea level (a.s.l.)), surrounded by semideciduous forest, compared with the other collection sites.[58] Inselberg species composition is strongly shaped by temperature and altitude, which are closely related to UV exposure, as plants growing at lower elevations experience reduced UV radiation.[58,59] Morphologically, *C. argenteus* exhibits specialized structures, with its body heavily covered by whitish and greyish trichomes and leaves appressed along the trunk (according to Monge *et al.*),[17] which may help mitigate the effects of high temperatures by reflecting light and reducing water loss through evaporation.[59] Additionally, *C. argenteus* seems to occur in larger vegetation mats (according to Monge *et al.*),[17] where nutrients are often more abundant. The interaction between these environmental conditions and plant traits may drive metabolic adaptations in *C. argenteus* toward more conservative and classical chemical defense strategies, resulting in a less diverse chemical profile.

In contrast, *C. longiangustatus* and *C. rupestris* were collected in the central region of the state (19°47'49.0"S, 40°46'31.0"W and 19°58'17.0"S, 40°31'49.0"W, respectively) in a relatively high-altitude area (1,019 m a.s.l. and 944 m a.s.l., respectively) characterized by a wetter climate, lower mean annual temperature (16-18 °C), and surrounded by dense montane ombrophylous forest.[60] Both species exhibited similar chemical profiles in terms of metabolite richness and diversity (i.e., both species presented comparable numbers of flavonoids and sesquiterpene lactones). However, *C. longiangustatus* exhibited higher content of hydroxycinnamic acid derivatives. In terms of microhabitats, high-altitude inselbergs are considered even harsher environments, characterized by nutrient-

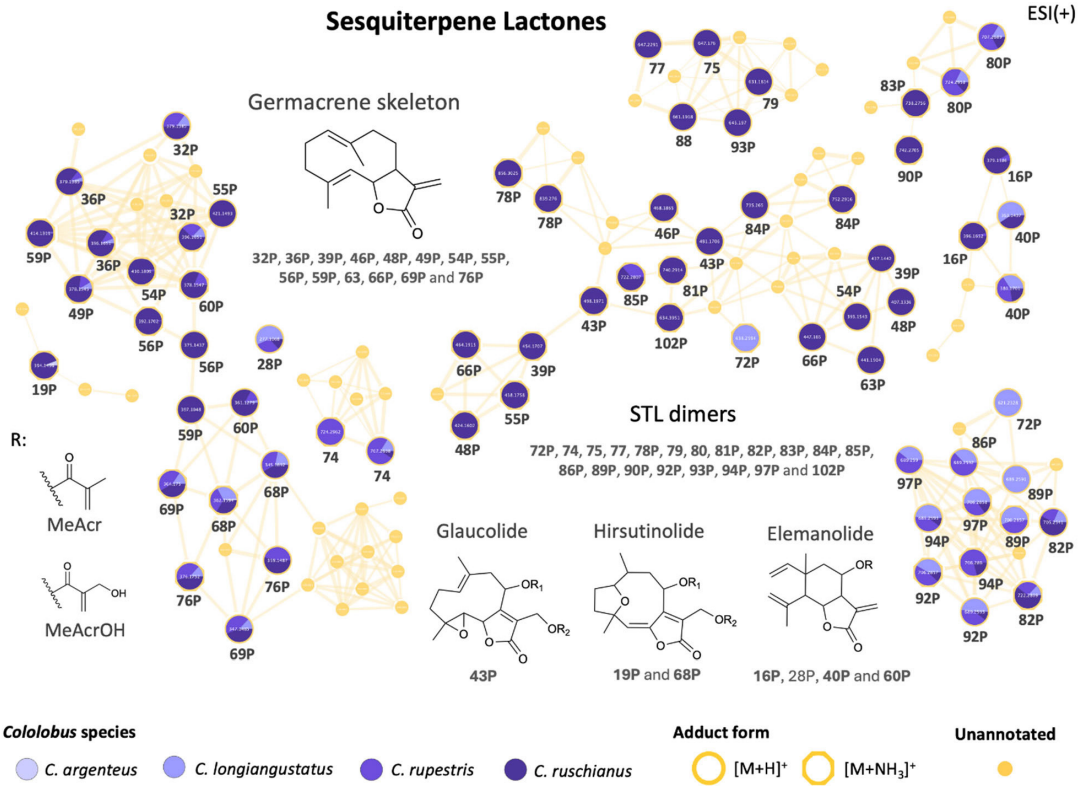

Figure 5. LC-MS/MS molecular networking of *Cololobus* species in the negative ionization mode, highlighting the cluster of metabolites classified as sesquiterpene lactones.

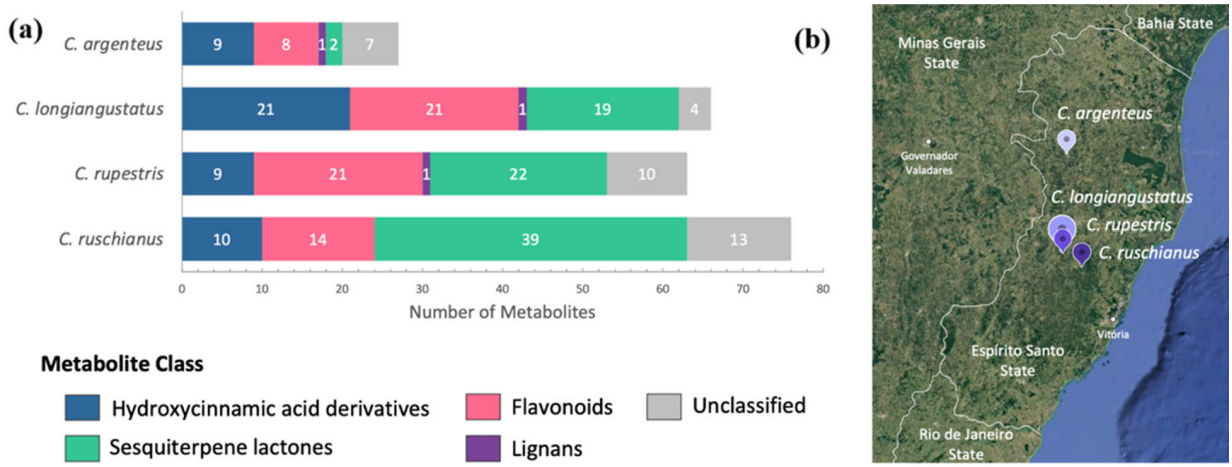

Figure 6. Metabolite richness, measured as the number of metabolites, across *Cololobus* species classified as hydroxycinnamic acid derivatives, flavonoids, lignans, and sesquiterpene lactones or remained unclassified (a). Map showing the geographical locations where *Cololobus* species were collected (b).

poor soils, high UV radiation, strong winds, limited water availability, and substantial daily temperature fluctuations.[61] Both species, *C. longiangustatus* and *C. rupestris*, exhibit putative adaptations to these harsh conditions, such as dense trichomes on the leaves, deciduous leaves, appressed leaves to the trunks.[17] Indeed, considering the environmental harshness of high-altitude inselbergs, the metabolism of *C. longiangustatus* and *C. rupestris* appears to be shaped toward a more complex chemical response, thereby promoting the production of more diverse metabolites.

C. ruschianus was also collected in the central region of the state (19°54'40"S, 40°36'09"W), but at an intermediate altitude site (611 m a.s.l.) compared to the other sampling sites. This population of *C. ruschianus* was found in a rock crack, with almost no soil and no other plant forming vegetation mats, on a very steep inclination (above 70°), within a 250-300 m-deep valley (according to Monge *et al.*).[16] Compared with the other collection sites, this location represents an even harsher inselberg microhabitat, as winds are expected to be stronger and water and nutrients less available, while UV radiation incidence is expected to be intermediate. Among the analyzed species, we observed that *C. ruschianus* exhibited the greatest diversity of sesquiterpene lactones, resulting in greater overall metabolite richness. Such diversity may reflect the activation of more complex chemical defense strategies to cope with extremely severe environmental conditions.

Upon comparing the chemical profiles across *Cololobus* species, we observed that *C. longiangustatus* possesses a richer set of hydroxycinnamic acid derivatives, exhibiting nearly twice as many of these metabolites as the other species. Likewise, when evaluating the distribution of sesquiterpene lactones among the *Cololobus* species, we found that *C. ruschianus* exhibits a markedly enriched profile, presenting approximately twice the number of such metabolites compared to the remaining species. Differences in microhabitat strongly influence the plant community, shaping metabolic responses to environmental stress.[11] *Cololobus* species collected in harsher microhabitats, exhibited more complex and diverse chemical profiles (*C. ruschianus*), whereas those from less stressful microhabitats exhibited less diverse chemical profiles (*C. argenteus*). Additionally, geographical location data showed that metabolite richness may be associated with the elevation at which plants were growing. *Cololobus* species collected at higher and intermediate altitudes, between 600 and 1050 m a.s.l., exhibited more complex and diverse chemical profiles (*C. longiangustatus, C. rupestris,* and *C. ruschianus*), whereas those collected at lower altitudes exhibited less diverse chemical profiles (*C. argenteus*). This trend may reflect enhanced chemical defense strategies in response to stressful and harsher inselberg microhabitat conditions.

Conclusions

Comparative chemical profiles of *Cololobus* species revealed a high prevalence of phenolic compounds, including hydroxycinnamic acid derivatives and flavonoids, and sesquiterpene lactones. Interestingly, *C. argenteus* exhibited a less diverse chemical profile, with fewer detectable metabolites, suggesting a more conserved metabolism or reduced chemical defense strategies for coping with environmental challenges. By contrast, *C. longiangustatus*, *C. ruschianus*, and *C. rupestris* displayed more complex metabolic repertoires, consistent with broader or more flexible ecological strategies, maybe in response to harsher microhabitats. Such interspecific differences in chemical diversity highlight the potential adaptive roles of specialized metabolites in shaping ecological adaptations within the genus.

Supplementary Information

Supplementary Information is available free of charge at http://jbcs.sbq.org.br as PDF file.

Data Availability Statement

All raw LC-MS/MS data (.lcd and .mzXML files), along with the processed data (.mgf files and .csv spreadsheets) employed for molecular networking and SIRIUS predictions, were deposited at the Mass Spectrometry Interactive Virtual Environment (MassIVE) website. The dataset is publicly available at the MassIVE website (http://massive.ucsd.edu) under the identifier MSV000100566 [https://doi.org/10.25345/C5CV4C54S].

Acknowledgments

The authors acknowledge FAPESP (grants No. 2023/18392-4, No. 2020/02207-5, No. 2024/02286-3, No. 2024/03447-0, No. 2024/15360-7), FAPEMIG (APQ No. 00525-21), INCT Nature (No. 408549/2024-6), CNPq, and CAPES (code 001) for financial support.

Author Contributions

M. E. G., M. M. and N. P. L designed the study; M. E. G. carried out the experiments, performed data analyses and manual curation; M. M. contributed to sample collection; M. E. G and M. M. draft the manuscript. All authors reviewed and approved the final manuscript.

References

1. The Brazil Flora Group; *Rodriguesia* **2015**, *66*, 1085. [Crossref]
2. Morellato, L. P. C.; Haddad, C. F. B.; *Biotropica* **2018**, *32*, 786. [Crossref]
3. Marques, M. C. M.; Trindade, W.; Bohn, A.; Grelle, C. E. V. In *The Atlantic Forest: History, Biodiversity, Threats and Opportunities of the Mega-Diverse Forest*; Marques, M. C. M.; Grelle, C. E. V., eds.; Springer International Publishing: Cham, Switzerland, 2021. [Crossref]
4. Myers, N.; Mittermeier, R. A.; Mittermeier, C. G.; da Fonseca, G. A. B; Kent, J.; *Nature* **2000**, *403*, 853. [Crossref]
5. Rezende, C. L.; Scarano, F. R.; Assad, E. D.; Joly, C. A.; Metzger, J. P.; Strassburg, B. B. N.; Tabarelli, M.; Fonseca, G. A.; Mittermeier, R. A.; *Perspect. Ecol. Conserv.* **2018**, *16*, 208. [Crossref]
6. Carnaval, A. C.; Waltari, E.; Rodrigues, M. T.; Rosauer, D.; VanDerWal, J.; Damasceno, R.; Prates, I.; Strangas, M.; Spanos, Z.; Rivera, D.; Pie, M. R.; Firkowski, C. R.; Bornschein, M. R.; Ribeiro, L. F.; Moritz, C.; *Proc. R. Soc. B* **2014**, *281*, 20141461. [Crossref]
7. Couto, D. R.; Dan, M. L.; Aguiar, W. M.; Braga, J. M. A.; Nascimento, M. T.; *Rodriguesia* **2021**, *72*, e00872020. [Crossref]
8. Barbosa-Silva, R. G.; Andrino, C. O.; Azevedo, L.; Lucresia, L.; Lovo, J.; Hiura, A. L.; Viana, P. L.; Giannini, T. C.; Zappi, D. C.; *Front. Plant Sci.* **2022**, *13*, 928577. [Crossref]
9. de Paula, L. F. A.; Mota, N. F. O.; Viana, P. L.; Stehmann, J. R.; *Acta Bot. Bras.* **2017**, *31*, 199. [Crossref]
10. Tabarelli, M.; Pinto, L. P.; Silva, J. M. C.; Hirota, M.; Bedê, L.; *Conserv. Biol.* **2005**, *19*, 695. [Crossref]
11. Vanschoenwinkel, B.; de Paula, L. F. A.; Snoeks, J. M.; der Stocken, T. V.; Buschke, F. T.; Porembski, S.; Silveira, F. A. O.; *Biol. Rev.* **2025**, *100*, 481. [Crossref]
12. Sabino, G. P.; Pinheiro, F.; Cabral, J. S.; Koch, I.; Marcusso, G. M.; Tavares, M. M.; Cunha, I. M.; Kamimura, V. A.; *J. Veg. Sci.* **2025**, *36*, e70037. [Crossref]
13. Robinson, H.; *Smithson. Contrib. Bot.* **1999**, *89*, 1932. [Crossref]
14. Robinson, H. In *The Families and Genera of Vascular Plants*; Kadereit, W.; Jeffrey, C., eds.; Springer: Berlin, Germany, 2007.
15. Robinson, H.; *Proc. Biol. Soc. Wash.* **1994**, *107*, 557. [Link] accessed in March 2026
16. Monge, M.; Fontana, A. P.; de Fraga, C. N.; Kollmann, L. J. C.; Nakajima, J. N.; *Syst. Bot.* **2021**, *46*, 1114. [Crossref]
17. Monge, M.; Volet, D. P.; Semir, J.; *Rodriguesia* **2018**, *69*, 595. [Crossref]
18. Ernst, M.; Silva, D. B.; Silva, R.; Monge, M.; Semir, J.; Vêncio, R. Z. N.; Lopes, N. P.; *Anal. Chim. Acta* **2015**, *859*, 46. [Crossref]
19. Martucci, M. E. P.; De Vos, R. C. H.; Carollo, C. A.; Gobbo-Neto, L.; *PLoS One* **2014**, *9*, e93149. [Crossref]
20. Gallon, M. E.; Monge, M.; Casoti, R.; da Costa, F. B.; Semir, J.; Gobbo-Neto, L.; *Phytochemistry* **2018**, *150*, 93.[Crossref]
21. Peters, K.; Worrich, A.; Weinhold, A.; Alka, O.; Balcke, G.; Birkemeyer, C.; Bruelheide, H.; Calf, O. W.; Dietz, S.; Dührkop, K.; Gaquerel, E.; Heinig, U.; Kücklich, M.; Macel, M.; Müller, C.; Poeschl, Y.; Pohnert, G.; Ristok, C.; Rodríguez, V. M.; Ruttkies, C.; Schuman, M.; Schweiger, R. Shahaf, N.; Steinbeck, C.; Tortosa, M.; Treutler, H.; Ueberschaar, N.; Velasco, P.; Weiß, B. M.; Widdig, A.; Neumann, S.; van Dam, N. M.; *Int. J. Mol. Sci.* **2018**, *19*, 1385. [Crossref]
22. Salam, U.; Ullah, S.; Tang, Z. H.; Elateeq, A. A.; Khan, Y.; Khan, J.; Khan, A.; Ali, S.; *Life* **2023**, *13*, 706. [Crossref]
23. Carrera, F. P.; Noceda, C.; Maridueña-Zavala, M. G.; Cevallos-Cevallos, J. M.; *Agronomy* **2021**, *11*, 824. [Crossref]
24. Shah, A. K. P.; Walter, A.; Ottosson, F.; Russo, F.; Navarro-Diaz, M.; Boldt, J.; Kalinski, J. C. J.; Kontou, E. E.; Elofson, J.; Polyzois, A.; González-Marín, C.; Farrell, S.; Aggerbeck, M. R.; Pruksatrakul, T.; Chan, N.; Wang, Y.; Pöchhacker, M.; Brungs, C.; Cámara, B.; Caraballo-Rodríguez, A. M.; Cumsille, A.; de Oliveira, F.; Dührkop, K.; El Abiead, Y.; Geibel, C.; Graves,

L. G.; Hansen, M.; Heuckeroth, S.; Knoblauch, S.; Kostenko, A.; Kuijpers, M. C. M.; Mildau, K.; Lambidis, S. P.; Gomes, P. W. P.; Schramm, T.; Steuer-Lodd, K.; Stincone, P.; Tayyab, S.; Vitale, G. A.; Wagner, B. C.; Xing, S.; Yazzie, M. T.; Zuffa, S.; de Kruijff, M.; Beemelmanns, C.; Link, H.; Mayer, C.; van der Hooft, J. J. J.; Damiani, T.; Pluskal, T.; Dorrestein, P.; Stanstrup, J.; Schmid, R.; Wang, M.; Aron, A.; Ernst, M.; Petras, D.; *Nat. Protoc.* **2025**, *20*, 92. [Crossref]

25. David, P. A.; Norazhar, A. I.; Che Zain, M. S.; *J. Sep. Sci.* **2025**, *48*, e70230. [Crossref]
26. de Vos, R. C. H.; Moco, S.; Lommen, A.; Keurentjes, J. J. B.; Bino, R. J.; Hall, R. D.; *Nat. Protoc.* **2007**, *2*, 778. [Crossref]
27. Fiehn, O.; *Plant Mol. Biol.* **2002**, *48*, 155. [Crossref]
28. Dunn, W. B.; Ellis, D. I.; *TrAC, Trends Anal. Chem.* **2005**, *24*, 285. [Crossref]
29. Sumner, L. W.; Amberg, A.; Barrett, D.; Beale, M. H.; Beger, R.; Daykin, C. A.; Fan, T. W. M.; Fiehn, O.; Goodacre, R.; Griffin, J. L.; Hankemeier, T.; Hardy, N.; Harnly, J.; Higashi, R.; Kopka, J.; Lane, A. N.; Lindon, J. C.; Marriott, P.; Nicholls, A. W.; Reily, M. D.; Thaden, J. J.; Viant, M. R.; *Metabolomics* **2007**, *3*, 211. [Crossref]
30. Blaženović, I.; Kind, T.; Ji, J.; Fiehn, O.; *Metabolites* **2018**, *8*, 31. [Crossref]
31. Nothias, L. F.; Petras, D.; Schmid, R.; Dührkop, K.; Rainer, J.; Sarvepalli, A.; Protsyuk, I.; Ernst, M.; Tsugawa, H.; Fleischauer, M.; Aicheler, F.; Aksenov, A. A.; Alka, O.; Allard, P. M.; Barsch, A.; Cachet, X.; Caraballo-Rodriguez, A. M.; da Silva, R. R.; Dang, T.; Garg, N.; Gauglitz, J. M.; Gurevich, A.; Isaac, G.; Jarmusch, A. K.; Kameník, Z.; Kang, K. B.; Kessler, N.; Koester, I.; Korf, A.; Le Gouellec, A.; Ludwig, M.; Martin H. C.; McCall, L. I.; McSayles, J.; Meyer, S. W.; Mohimani, H.; Morsy, M.; Moyne, O.; Neumann, S.; Neuweger, H.; Nguyen, N. H.; Nothias-Esposito, M.; Paolini, J.; Phelan, V. V.; Pluskal, T.; Quinn, R. A.; Rogers, S.; Shrestha, B.; Tripathi, A.; van der Hooft, J. J. J.; Vargas, F.; Weldon, K. C.; Witting, M.; Yang, H.; Zhang, Z.; Zubeil, F.; Kohlbacher, O.; Böcker, S.; Alexandrov, T.; Bandeira, N.; Wang, M.; Dorrestein, P. C.; *Nat. Methods* **2020**, *17*, 905. [Crossref]
32. Wang, M.; Carver, J. J.; Phelan, V. V.; Sanchez, L. M.; Garg, N.; Peng, Y.; Nguyen, D. D.; Watrous, J.; Kapono, C. A.; Luzzatto-Knaan, T.; Porto, C.; Bouslimani, A.; Melnik, A. V.; Meehan, M. J.; Liu, W. T.; Crüsemann, M.; Boudreau, P. D.; Esquenazi, E.; Sandoval-Calderón, M.; Kersten, R. D.; Pace, L. A.; Quinn, R. A.; Duncan, K. R.; Hsu, C. C.; Floros, D. J.; Gavilan, R. G.; Kleigrewe, K.; Northen, T.; Dutton, R. J.; Parrot, D.; Carlson, E. E.; Aigle, B.; Michelsen, C. F.; Jelsbak, L.; Sohlenkamp, C.; Pevzner, P.; Edlund, A.; McLean, J.; Piel, J.; Murphy, B. T.; Gerwick, L.; Liaw, C. C.; Yang, Y. L.; Humpf, H. U.; Maansson, M.; Keyzers, R. A.; Sims, A. C.; Johnson, A. R.; Sidebottom, A. M.; Sedio, B. E.; Klitgaard, A.; Larson, C. B.; Boya P., C. A.; Torres-Mendoza, D.; Gonzalez, D. J.; Silva, D. B.; Marques, L. M.; Demarque, D. P.; Pociute, E.; O'Neill, E. C.; Briand, E.; Helfrich, E. J. M.; Granatosky, E. A.; Glukhov, E.; Ryffel, F.; Houson, H.; Mohimani, H.; Kharbush, J. J.; Zeng, Y.; Vorholt, J. A.; Kurita, K. L.; Charusanti, P.; McPhail, K. L.; Nielsen, K. F.; Vuong, L.; Elfeki, M.; Traxler, M. F.; Engene, N.; Koyama, N.; Vining, O. B.; Baric, R.; Silva, R. R.; Mascuch, S. J.; Tomasi, S.; Jenkins, S.; Macherla, V.; Hoffman, T.; Agarwal, V.; Williams, P. G.; Dai, J.; Neupane, R.; Gurr, J.; Rodríguez, A. M. C.; Lamsa, A.; Zhang, C.; Dorrestein, K.; Duggan, B. M.; Almaliti, J.; Allard, P. M.; Phapale, P.; Nothias, L. F.; Alexandrov, T.; Litaudon, M.; Wolfender, J. L.; Kyle, J. E.; Metz, T. O.; Peryea, T.; Nguyen, D. T.; VanLeer, D.; Shinn, P.; Jadhav, A.; Müller, R.; Waters, K. M.; Shi, W.; Liu, X.; Zhang, L.; Knight, R.; Jensen, P. R.; Palsson, B. Ø.; Pogliano, K.; Linington, R. G.; Gutiérrez, M.; Lopes, N. P.; Gerwick, W. H.; Moore, B. S.; Dorrestein, P. C.; Bandeira, N.; *Nat. Biotechnol.* **2016**, *34*, 828 [Crossref]; Global Natural Product Social Molecular Networking (GNPS). [Link] accessed in March 2026
33. Thiers, B.; *Index Herbariorum: A Global Directory of Public Herbaria and Associated Staff*; New York Botanical Garden, 2025. [Link] accessed in March 2026
34. Thiers, B.; *The World's Herbaria 2019: A Summary Report Based on Data from Index Herbariorum*, 2020 [Link] accessed in March 2026
35. Happi, G. M.; Sikam, K. G.; Wansi, J. D.; Teufel, R.; *Phytochem. Rev.* **2025**, *24*, 5995. [Crossref]
36. Lopes, J. L.; *Mem. Inst. Oswaldo Cruz* **1991**, *86*, 227. [Crossref]
37. Bohlmann, F.; Muller, L.; Gupta, R. K.; King, R. M.; Robinson, H.; *Phytochemistry* **1981**, *20*, 2233. [Crossref]
38. Bohlmann, F.; Zdero, C.; King, R. M.; Robinson, H.; *Phytochemistry* **1982**, *21*, 695. [Crossref]
39. Jakupovic, J.; Schmeda-hirschmann, G.; Schuster, A.; Zdero, C.; Bohlmann, F.; King, R. M.; Robinson, H.; Pickardt, J.; *Phytochemistry* **1986**, *25*, 145. [Crossref]
40. Igual, M. O.; Martucci, M. E. P.; da Costa, F. B.; Gobbo-Neto, L.; *Biochem. Syst. Ecol.* **2013**, *51*, 94. [Crossref]
41. Lusa, M. G.; Martucci, M. E. P.; Loeuille, B. F. P.; Gobbo-Neto, L.; Appezzato-da-Glória, B.; da Costa, F. B.; *Bot. J. Linn. Soc.* **2016**, *182*, 594. [Crossref]
42. Gallon, M. E.; Jaiyesimi, O. A.; Gobbo-Neto, L.; *Biochem. Syst. Ecol.* **2018**, *78*, 5. [Crossref]
43. Bohlmann, F.; Jakupovic, J.; *Progress in the Chemistry of the Vernonieae (Compositae)*; Mabry, T. J.; Wagenitz, G., eds.; Springer: Vienna, Austria, 1990.
44. Taniguchi, M.; LaRocca, C. A.; Bernat, J. D.; Lindsey, J. S.; *J. Nat. Prod.* **2023**, *86*, 1087. [Crossref]
45. Gobbo-Neto, L.; Lopes, N. P.; *J. Agric. Food Chem.* **2008**, *56*, 1193. [Crossref]
46. Clifford, M. N.; Knight, S.; Kuhnert, N.; *J. Agric. Food Chem.* **2005**, *53*, 3821. [Crossref]

47. Clifford, M. N.; Johnston, K. L.; Knight, S.; Kuhnert, N.; *J. Agric. Food Chem.* **2003**, *51*, 2900. [Crossref]
48. Meng, X.; Lv, H.; Ding, X. Q.; Jian, T. Y.; Guo, D. I.; Feng, X. J.; Ren, B. R.; Chen, J.; *Phytochemistry* **2022**, *203*, 113377. [Crossref]
49. Michalska, K.; Stojakowska, A.; Malarz, J.; Doležalová, I.; Lebeda, A.; Kisiel, W.; *Biochem. Syst. Ecol.* **2009**, *37*, 174. [Crossref]
50. da Silva, L. A. L.; Sandjo, L. P.; Misturini, A.; Caramori, G. F.; Biavatti, M. W.; *J. Mass Spectrom.* **2019**, *54*, 915. [Crossref]
51. Crotti, A. E. M.; Lopes, J. L. C.; Lopes, N. P.; *J. Mass Spectrom.* **2005**, *40*, 1030. [Crossref]
52. Gobbo-Neto, L.; Bauermeister, A.; Sakamoto, H.; Gouvea, D. R.; Lopes, J. L. C.; Lopes, N. P.; *J. Braz. Chem. Soc.* **2017**, *28*, 2382. [Crossref]
53. Gobbo-Neto, L.; Guaratini, T.; Pessoa, C.; de Moraes, M. O.; Costa-Lotufo, L. V.; Vieira, R. F.; Colepicolo, P.; Lopes, N. P.; *J. Braz. Chem. Soc.* **2010**, *21*, 750. [Crossref]
54. Gouvea, D. R.; Gobbo-Neto, L.; Sakamoto, H. T.; Lopes, N. P.; *Quim. Nova* **2012**, *35*, 2139. [Crossref]
55. Sakamoto, H. T.; Gobbo-Neto, L.; Cavalheiro, A. J.; Lopes, N. P.; Lopes, J. L. C.; *J. Braz. Chem. Soc.* **2005**, *16*, 1396. [Crossref]
56. Gouvea, D. R.; Meloni, F.; Ribeiro, A. B. B.; Lopes, J. L. C.; Lopes, N. P.; *Anal. Chim. Acta* **2012**, *748*, 28. [Crossref]
57. Keles, L. C.; de Melo, N. I.; Aguiar, G. P.; Wakabayashi, K. A. L.; de Carvalho, C. E.; Cunha, W. R.; Crotti, A. E. M.; Lopes, J. L. C.; Lopes, N. P.; *Quim. Nova* **2010**, *33*, 2245. [Crossref]
58. Pinto-Jr., H. V.; Villa, P. M.; de Menezes, L. F. T.; Pereira, M. C. A.; *J. Mt. Sci.* **2020**, *17*, 1931. [Crossref]
59. Porembski, S.; Barthlott, W.; *Inselbergs: Biotic Diversity of Isolated Rock Outcrops in Tropica and Temperate Regions*, 1st ed.; Springer: Berlin, Germany, 2000. [Crossref]
60. Esgario, C. P.; Ribeiro, L. F.; Silva, A. G.; *Natureza Online* **2008**, *6*, 55. [Crossref]
61. Hopper, S. D.; Lambers, H.; Silveira, F. A. O.; Fiedler, P. L.; *Biol. J. Linn. Soc.* **2021**, *133*, 266. [Crossref]

Submitted: December 8, 2025
Final version online: March 18, 2026